Physics Procedia

Volume 75, 2015, Pages 206–213

20th International Conference on Magnetism

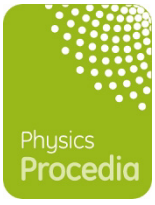

# Doping-induced states in the single-particle spectrum originating from magnetic excitation of a Mott insulator

Masanori Kohno

WPI Center for Materials Nanoarchitectonics,
National Institute for Materials Science, Tsukuba 305-0044, Japan
KOHNO.Masanori@nims.go.jp

**Abstract**

By infinitesimal doping of a Mott insulator, states are induced in the Mott gap in the single-particle spectrum. To clarify the nature of these states, their relationships with the magnetically excited states of the Mott insulator are investigated. By using the commutator between the Hamiltonian and an electron creation operator of the $t$-$J$ model, it is shown that the doping-induced states generally have considerable overlaps with the magnetically excited states of the Mott insulator. In addition, the electron-addition spectral weight of spin-1 states from the spin-1/2 ground state is shown to be three times as large as that of spin-0 states in the $t$-$J$ model. These results imply that the doping-induced states in the small-doping limit of a continuous Mott transition can generally be interpreted as essentially the magnetically excited states of the Mott insulator which exhibit the momentum-shifted magnetic dispersion relation primarily outside the free-electron Fermi surface in the electron-addition spectrum following the doping. This picture is supported by numerical results for the one- and two-dimensional $t$-$J$ models.

*Keywords:* Mott transition, doping-induced states, magnetic excitation, $t$-$J$ model

## 1 Introduction

The single-particle spectrum of a Mott insulator appears similar to that of a conventional band insulator: an energy gap opens, and the chemical potential is located in the gap. However, when the chemical potential touches the lower Hubbard band (LHB) by lowering the chemical potential, a significant difference appears: states which do not exist in the single-particle spectrum of the Mott insulator emerge in the Mott gap [1, 2]. Thus, the single-particle spectrum drastically changes from that of the Mott insulator although the spectral weights of the emergent states are very small when the doping concentration is very small. This characteristic is due to strong electronic correlations and must be related to the nature of the Mott transition. These states, which are called doping-induced states or ingap states, have been observed in various materials such as cuprate high-temperature superconductors [3, 4, 5, 6, 7], but their interpretations are controversial.



Selection and peer-review under responsibility of the Scientific Programme Committee of ICM 2015



doi:10.1016/j.phpro.2015.12.026

A popular interpretation of these states is that the relaxation of binding between double occupancy and vacancy induces states in the Mott gap following the doping of a Mott insulator [8, 9, 10, 11, 12]. In this interpretation, the doping-induced states are considered to be essentially disconnected from the lower-energy states by an energy gap due to the weak binding between double occupancy and vacancy [8]. A considerable number of theoretical results not only for the two-dimensional (2D) Hubbard model but also for the 2D $t$-$J$ model have suggested such a (pseudo)gap, which has been interpreted in terms of various concepts, such as the binding between double occupancy and vacancy [8, 9, 10, 11, 12], the effect of a charge $2e$ boson [11, 12], hybridization between the quasiparticle and cofermion [9, 10], and a spin-polaron shakeoff [13, 14].

Recently, another interpretation suggesting a gapless mode of the doping-induced states in the 2D Hubbard and $t$-$J$ models has been proposed: the magnetically excited states of the Mott insulator emerge in the single-particle spectrum with the dispersion relation shifted by the Fermi momentum following the doping of the Mott insulator [15, 16, 17, 18, 19]. In this interpretation, if the magnetic excitation is gapless in the Mott insulator, the mode of the doping-induced states is also gapless and exhibits the momentum-shifted magnetic (spin-wave) dispersion relation [15, 16, 17, 18, 20]. This picture is consistent with the recent numerical results for the 2D Hubbard and $t$-$J$ models in Refs. [15, 17] as well as with the results for the one-dimensional (1D) Hubbard model in Ref. [20]. In addition, this picture has been explicitly confirmed in the two-leg ladder and bilayer $t$-$J$ models in the limit of strong interchain and interplane couplings, respectively [18], and has been supported by a general argument on the quantum numbers and the overlaps of relevant states in the small-doping limit [18].

In this paper, to clarify the nature of the doping-induced states in the small-doping limit of a continuous Mott transition, the overlaps between the doping-induced states in the small-doping limit and the magnetically excited states of the Mott insulator at half-filling as well as the ratio between the electron-addition spectral weights of the spin-0 and spin-1 states from the spin-1/2 ground state are investigated in the $t$-$J$ model. The spectral functions of the 1D and 2D $t$-$J$ models are also studied numerically. The number of sites, which is assumed to be even, and the number of doped holes are denoted by $N_{\rm s}$ and $N_{\rm h}$, respectively. At half-filling, the doping concentration $\delta(=N_{\rm h}/N_{\rm s})$ is zero. The ground state in the small-doping limit is assumed to be a metallic state without phase separation.

## 2 Single-particle spectral function and quantum numbers

We study the single-particle spectral function at zero temperature defined as follows:

$$A(\boldsymbol{k},\omega)=\begin{cases} \frac{1}{2}\sum_{\sigma=\pm1/2}\sum_{m}|\langle m|c^{\dagger}_{\boldsymbol{k},\sigma}|{\rm GS}\rangle_h|^2\delta(\omega-\varepsilon_m) & \text{for} \quad \omega>0, \\ \frac{1}{2}\sum_{\sigma=\pm1/2}\sum_{m}|\langle m|c_{\boldsymbol{k},\sigma}|{\rm GS}\rangle_h|^2\delta(\omega+\varepsilon_m) & \text{for} \quad \omega<0, \end{cases}$$

where $|{\rm GS}\rangle_h$ denotes the ground state at $N_{\rm h}=h$, and $|m\rangle$ denotes an eigenstate with excitation energy $\varepsilon_m$ from $|{\rm GS}\rangle_h$. Here, $c^{\dagger}_{\boldsymbol{k},\sigma}$ denotes the creation operator of an electron with momentum $\boldsymbol{k}$ and magnetization $\sigma$. If $|{\rm GS}\rangle_h$ has spin $s$, magnetization $\varsigma$, and momentum $\boldsymbol{k}_{\rm F}$, $|\langle m|c^{(\dagger)}_{\boldsymbol{k},\sigma}|{\rm GS}\rangle_h|^2$ can be nonzero only for $|m\rangle$ at $N_{\rm h}=h+1$ $(h-1)$ with spin $|s\pm1/2|$, magnetization $\varsigma-\sigma$ $(\varsigma+\sigma)$, and momentum $\boldsymbol{k}_{\rm F}-\boldsymbol{k}$ $(\boldsymbol{k}_{\rm F}+\boldsymbol{k})$ because $c^{(\dagger)}_{\boldsymbol{k},\sigma}|{\rm GS}\rangle_h$ has components with these quantum numbers [18, 21]. In this paper, we particularly focus attention on the electron-addition excitation $(\omega>0)$ from the ground state at $N_{\rm h}=1$ $(|{\rm GS}\rangle_1)$. Then, $|\langle m|c^{\dagger}_{\boldsymbol{k},\sigma}|{\rm GS}\rangle_1|^2$ can be nonzero only for $|m\rangle$ at $N_{\rm h}=0$ with spin 0 or 1, magnetization $\varsigma+\sigma$ [13], and momentum $\boldsymbol{k}_{\rm F}+\boldsymbol{k}$ [18] if $|{\rm GS}\rangle_1$ has spin 1/2, magnetization $\varsigma$, and momentum $\boldsymbol{k}_{\rm F}$.

In interacting systems, $|\langle m|c^\dagger_{\boldsymbol{k},\sigma}|\mathrm{GS}\rangle_1|^2$ is generally expected to be nonzero if $|m\rangle$ has the same quantum numbers as those of components of $c^\dagger_{\boldsymbol{k},\sigma}|\mathrm{GS}\rangle_1$ for $\boldsymbol{k}$ where the LHB is not completely filled at $N_\mathrm{h}=1$. In particular, if $|m\rangle$ contributes to a dominant low-energy excitation at $N_\mathrm{h}=0$, $|\langle m|c^\dagger_{\boldsymbol{k},\sigma}|\mathrm{GS}\rangle_1|^2$ is expected to be relatively large [18]. Because the magnetic excitation is generally dominant at low energies in Mott insulators, states of the magnetic excitation should appear in $A(\boldsymbol{k},\omega)$ for $\omega>0$ in the small-doping limit with the dispersion relation shifted by the Fermi momentum for $\boldsymbol{k}$ where the LHB is not completely filled [18]. In the 1D and 2D $t$-$J$ and Hubbard models, because the gapless spin-wave mode is dominant at half-filling [22, 23], the doping-induced states in the small-doping limit should exhibit essentially the gapless spin-wave dispersion relation shifted by the Fermi momenta in the momentum region where the LHB is not completely filled [18]. This characteristic essentially agrees with the numerical results for the 1D and 2D Hubbard and 2D $t$-$J$ models in Refs. [15, 16, 17, 20].

## 3 Overlap

To strengthen the above argument, we consider the $t$-$J$ model defined by the following Hamiltonian:

$$\mathcal{H}=\sum_{i\neq j,\sigma}t_{i,j}\tilde{c}^\dagger_{i,\sigma}\tilde{c}_{j,\sigma}+\sum_{i\neq j}J_{i,j}(\boldsymbol{S}_i\cdot\boldsymbol{S}_j-\frac{1}{4}n_in_j)-\mu\sum_i n_i,$$

where $\tilde{c}_{i,\sigma}=c_{i,\sigma}(1-n_{i,-\sigma})$ and $n_i=\sum_\sigma n_{i,\sigma}$ for the annihilation operator $c_{i,\sigma}$ and number operator $n_{i,\sigma}$ of an electron with magnetization $\sigma$ at site $i$. Here, $\boldsymbol{S}_i$ denotes the spin operator at site $i$. In this model, although a vacant state $|0\rangle$ or a singly-occupied magnetization-$\sigma$ state $|\sigma\rangle$ is allowed at each site, double occupancy is forbidden. Here, we assume that $|\mathrm{GS}\rangle_0$ has spin 0 and momentum $\boldsymbol{0}$ and that $|\mathrm{GS}\rangle_1$ has spin 1/2, magnetization $\varsigma$, and momentum $\boldsymbol{k}_\mathrm{F}$.

The commutator $[\mathcal{H},\tilde{c}^\dagger_{\boldsymbol{k},\sigma}](=\mathcal{H}\tilde{c}^\dagger_{\boldsymbol{k},\sigma}-\tilde{c}^\dagger_{\boldsymbol{k},\sigma}\mathcal{H})$ is expressed [24] as

$$[\mathcal{H},\tilde{c}^\dagger_{\boldsymbol{k},\sigma}]=[\epsilon(\boldsymbol{k})-\mu]\tilde{c}^\dagger_{\boldsymbol{k},\sigma}+\frac{1}{\sqrt{N_\mathrm{s}}}\sum_i[\epsilon(\boldsymbol{k}_i)+\epsilon^\mathrm{S}(\boldsymbol{k}-\boldsymbol{k}_i)](S^{+,\sigma}_{\boldsymbol{k}-\boldsymbol{k}_i}\tilde{c}^\dagger_{\boldsymbol{k}_i,-\sigma}+S^{z,\sigma}_{\boldsymbol{k}-\boldsymbol{k}_i}\tilde{c}^\dagger_{\boldsymbol{k}_i,\sigma}-\frac{1}{2}n_{\boldsymbol{k}-\boldsymbol{k}_i}\tilde{c}^\dagger_{\boldsymbol{k}_i,\sigma}),\tag{1}$$

where $\tilde{c}^\dagger_{\boldsymbol{k},\sigma}=\frac{1}{\sqrt{N_\mathrm{s}}}\sum_j \mathrm{e}^{\mathrm{i}\boldsymbol{k}\cdot\boldsymbol{r}_j}\tilde{c}^\dagger_{j,\sigma}$, $S^{+(z),\sigma}_{\boldsymbol{k}}=\frac{1}{\sqrt{N_\mathrm{s}}}\sum_j \mathrm{e}^{\mathrm{i}\boldsymbol{k}\cdot\boldsymbol{r}_j}S^{+(z),\sigma}_j$, and $n_{\boldsymbol{k}}=\frac{1}{\sqrt{N_\mathrm{s}}}\sum_j \mathrm{e}^{\mathrm{i}\boldsymbol{k}\cdot\boldsymbol{r}_j}n_j$ using $S^{+,\sigma}_j=\tilde{c}^\dagger_{j,\sigma}\tilde{c}_{j,-\sigma}$, $S^{z,\sigma}_j=(n_{j,\sigma}-n_{j,-\sigma})/2$, and the site $j$ coordinate $\boldsymbol{r}_j$. Here, $\epsilon(\boldsymbol{k})$ and $\epsilon^\mathrm{S}(\boldsymbol{k})$ denote the Fourier transform of the hopping integral and that of the spin exchange coupling, respectively. In the 2D $t$-$J$ model, where $t_{i,j}$ and $J_{i,j}$ are nonzero only for neighboring sites on a square lattice (nonzero $t_{i,j}$ and $J_{i,j}$ are denoted by $-t$ and $J/2$, respectively; $t>0$ and $J>0$), $\epsilon(\boldsymbol{k})=-2t(\cos k_x+\cos k_y)$ and $\epsilon^\mathrm{S}(\boldsymbol{k})=J(\cos k_x+\cos k_y)$.

By using Eq. (1) and $n_{\boldsymbol{k}-\boldsymbol{k}'}|\mathrm{GS}\rangle_0=\sqrt{N_\mathrm{s}}\delta_{\boldsymbol{k},\boldsymbol{k}'}|\mathrm{GS}\rangle_0$ (because all sites are singly occupied at $N_\mathrm{h}=0$), we obtain the following relationship between ${}_0\langle\mathrm{GS}|\tilde{c}^\dagger_{-\boldsymbol{k}_\mathrm{F},-\varsigma}|\mathrm{GS}\rangle_1$ and the overlaps between the single-spin excited states at $N_\mathrm{h}=0$, $S^{+,\varsigma(z,-\varsigma)}_{\boldsymbol{k}_\mathrm{F}+\boldsymbol{k}}|\mathrm{GS}\rangle_0$, and the electron-addition states at $N_\mathrm{h}=1$, $\tilde{c}^\dagger_{\boldsymbol{k},\varsigma(-\varsigma)}|\mathrm{GS}\rangle_1$:

$$\begin{aligned}&[\mu_0-\frac{1}{2}\epsilon(-\boldsymbol{k}_\mathrm{F})+\frac{1}{2}\epsilon^\mathrm{S}(0)]{}_0\langle\mathrm{GS}|\tilde{c}^\dagger_{-\boldsymbol{k}_\mathrm{F},-\varsigma}|\mathrm{GS}\rangle_1\\&=\frac{1}{\sqrt{N_\mathrm{s}}}\sum_i[\epsilon(\boldsymbol{k}_i)+\epsilon^\mathrm{S}(-\boldsymbol{k}_\mathrm{F}-\boldsymbol{k}_i)]({}_0\langle\mathrm{GS}|S^{+,-\varsigma}_{-\boldsymbol{k}_\mathrm{F}-\boldsymbol{k}_i}\tilde{c}^\dagger_{\boldsymbol{k}_i,\varsigma}|\mathrm{GS}\rangle_1+{}_0\langle\mathrm{GS}|S^{z,-\varsigma}_{-\boldsymbol{k}_\mathrm{F}-\boldsymbol{k}_i}\tilde{c}^\dagger_{\boldsymbol{k}_i,-\varsigma}|\mathrm{GS}\rangle_1),\end{aligned}\tag{2}$$

where $\mu_0$ denotes the $\mu$ value that satisfies ${}_0\langle\mathrm{GS}|\mathcal{H}|\mathrm{GS}\rangle_0={}_1\langle\mathrm{GS}|\mathcal{H}|\mathrm{GS}\rangle_1$, which leads to ${}_0\langle\mathrm{GS}|[\mathcal{H},\tilde{c}^\dagger_{\boldsymbol{k},\sigma}]|\mathrm{GS}\rangle_1=0$. In the 2D $t$-$J$ model, $\epsilon(-\boldsymbol{k}_\mathrm{F})\approx 0$, and $\mu_0$ is typically $t\sim 2t$ in the

small-$J/t$ regime [17, 25]. Equation (2) implies that the overlaps between the single-spin excited states at $N_{\rm h}=0$ and the electron-addition states at $N_{\rm h}=1$ are $O(1/\sqrt{N_{\rm s}})$ at $O(N_{\rm s})$ $\boldsymbol{k}$ points primarily outside the free-electron Fermi surface [$\epsilon(\boldsymbol{k}) \gtrsim 0$] in the small-$J/t$ regime if ${}_0\langle {\rm GS}|\tilde{c}^{\dagger}_{-\boldsymbol{k}_{\rm F},-\varsigma}|{\rm GS}\rangle_1$ is $O(1)$. Because $\frac{1}{N_{\rm s}}\sum_i {}_0\langle {\rm GS}|\boldsymbol{S}_{-\boldsymbol{k}_i}\cdot\boldsymbol{S}_{\boldsymbol{k}_i}|{\rm GS}\rangle_0 = 3/4$ and $\frac{1}{N_{\rm s}}\sum_i {}_1\langle {\rm GS}|\tilde{c}_{\boldsymbol{k}_i,\sigma}\tilde{c}^{\dagger}_{\boldsymbol{k}_i,\sigma}|{\rm GS}\rangle_1 = 1/N_{\rm s}$ [26, 27], the overlaps between the normalized single-spin excited states $S^{+,\varsigma(z,-\varsigma)}_{\boldsymbol{k}_{\rm F}+\boldsymbol{k}}|{\rm GS}\rangle_0/\sqrt{{}_0\langle {\rm GS}|S^{+,-\varsigma(z,-\varsigma)}_{-\boldsymbol{k}_{\rm F}-\boldsymbol{k}}S^{+,\varsigma(z,-\varsigma)}_{\boldsymbol{k}_{\rm F}+\boldsymbol{k}}|{\rm GS}\rangle_0}$ and the normalized electron-addition states $\tilde{c}^{\dagger}_{\boldsymbol{k},\varsigma(-\varsigma)}|{\rm GS}\rangle_1/\sqrt{{}_1\langle {\rm GS}|\tilde{c}_{\boldsymbol{k},\varsigma(-\varsigma)}\tilde{c}^{\dagger}_{\boldsymbol{k},\varsigma(-\varsigma)}|{\rm GS}\rangle_1}$ should normally be $O(1)$ at these $\boldsymbol{k}$ points. This implies that the single-spin excited states at half-filling significantly contribute to the doping-induced states in the small-doping limit if ${}_0\langle {\rm GS}|\tilde{c}^{\dagger}_{-\boldsymbol{k}_{\rm F},-\varsigma}|{\rm GS}\rangle_1$ is $O(1)$.

In Ref. [18], a similar argument has been made based on the following relationships:

$$ {}_0\langle {\rm GS}|\tilde{c}^{\dagger}_{-\boldsymbol{k}_{\rm F},-\varsigma}|{\rm GS}\rangle_1 = \frac{1}{\sqrt{N_{\rm s}}}\sum_i {}_0\langle {\rm GS}|S^{+,-\varsigma}_{-\boldsymbol{k}_{\rm F}-\boldsymbol{k}_i}\tilde{c}^{\dagger}_{\boldsymbol{k}_i,\varsigma}|{\rm GS}\rangle_1 = \frac{2}{\sqrt{N_{\rm s}}}\sum_i {}_0\langle {\rm GS}|S^{z,-\varsigma}_{-\boldsymbol{k}_{\rm F}-\boldsymbol{k}_i}\tilde{c}^{\dagger}_{\boldsymbol{k}_i,-\varsigma}|{\rm GS}\rangle_1. \tag{3} $$

Although Eq. (2) leads to the same order estimation as that based on Eq. (3), we can eliminate the contribution at a specific $\boldsymbol{k}$ point by combining Eqs. (2) and (3):

$$ \begin{aligned} &[\mu_0 - \frac{1}{2}\epsilon(-\boldsymbol{k}_{\rm F}) + \frac{1}{2}\epsilon^{\rm S}(0) - \frac{3}{2}\gamma]{}_0\langle {\rm GS}|\tilde{c}^{\dagger}_{-\boldsymbol{k}_{\rm F},-\varsigma}|{\rm GS}\rangle_1 \\ &= \frac{1}{\sqrt{N_{\rm s}}}\sum_i [\epsilon(\boldsymbol{k}_i) + \epsilon^{\rm S}(-\boldsymbol{k}_{\rm F}-\boldsymbol{k}_i) - \gamma]({}_0\langle {\rm GS}|S^{+,-\varsigma}_{-\boldsymbol{k}_{\rm F}-\boldsymbol{k}_i}\tilde{c}^{\dagger}_{\boldsymbol{k}_i,\varsigma}|{\rm GS}\rangle_1 + {}_0\langle {\rm GS}|S^{z,-\varsigma}_{-\boldsymbol{k}_{\rm F}-\boldsymbol{k}_i}\tilde{c}^{\dagger}_{\boldsymbol{k}_i,-\varsigma}|{\rm GS}\rangle_1). \end{aligned} \tag{4} $$

For instance, the contribution from ${}_0\langle {\rm GS}|S^{+(z),-\varsigma}_{\boldsymbol{\pi}}\tilde{c}^{\dagger}_{-\boldsymbol{k}_{\rm F}-\boldsymbol{\pi},\varsigma(-\varsigma)}|{\rm GS}\rangle_1$ can be eliminated if $\gamma$ is set to $\epsilon(-\boldsymbol{k}_{\rm F}-\boldsymbol{\pi})+\epsilon^{\rm S}(\boldsymbol{\pi})$. Thus, even if the spin correlation at the antiferromagnetic momentum $\boldsymbol{\pi}$, ${}_0\langle {\rm GS}|S^{+,-\varsigma(z,-\varsigma)}_{\boldsymbol{\pi}}S^{+,\varsigma(z,-\varsigma)}_{\boldsymbol{\pi}}|{\rm GS}\rangle_0$, is very large, Eq. (4) with $\gamma=\epsilon(-\boldsymbol{k}_{\rm F}-\boldsymbol{\pi})+\epsilon^{\rm S}(\boldsymbol{\pi})$ implies that the contributions from ${}_0\langle {\rm GS}|S^{+(z),-\varsigma}_{-\boldsymbol{k}_{\rm F}-\boldsymbol{k}}\tilde{c}^{\dagger}_{\boldsymbol{k},\varsigma(-\varsigma)}|{\rm GS}\rangle_1$ for $-\boldsymbol{k}_{\rm F}-\boldsymbol{k}\neq\boldsymbol{\pi}$ continue to be $O(1/\sqrt{N_{\rm s}})$ at $O(N_{\rm s})$ $\boldsymbol{k}$ points primarily outside the free-electron Fermi surface [$\epsilon(\boldsymbol{k})\gtrsim 0$] in the small-$J/t$ regime.

In 1D systems, even if ${}_0\langle {\rm GS}|\tilde{c}^{\dagger}_{-\boldsymbol{k}_{\rm F},-\varsigma}|{\rm GS}\rangle_1 \to 0$ for $N_{\rm s}\to 0$, the doping-induced states in the small-doping limit can be essentially identified with the states of the dominant part of the magnetic excitation [Fig. 1(a)] (Sec. 5) [16, 18, 20, 28].

# 4 Spectral weights of spin-singlet and spin-triplet states

As mentioned in Sec. 2, spin-0 and spin-1 states are obtained by adding an electron to the spin-1/2 ground state. In this section, we consider how large the spectral weight of the spin-1 states is in comparison with that of the spin-0 states.

By adding an electron with magnetization $\varsigma$ to the spin-1/2 and magnetization-$\varsigma$ ground state, a spin-1 and magnetization-$2\varsigma$ state is obtained; only spin-1 states with magnetization-$2\varsigma$ of the Heisenberg model can appear in the spectral function for $\tilde{c}^{\dagger}_{\boldsymbol{k},\varsigma}|{\rm GS}\rangle_1$ if $|{\rm GS}\rangle_1$ has spin 1/2 and magnetization $\varsigma$ in the $t$-$J$ model. By noting that $\frac{1}{N_{\rm s}}\sum_i {}_h\langle {\rm GS}|\tilde{c}_{\boldsymbol{k}_i,\sigma}\tilde{c}^{\dagger}_{\boldsymbol{k}_i,\sigma}|{\rm GS}\rangle_h = h/N_{\rm s}(=\delta)$ [26, 27] regardless of the value of $\sigma$ and by considering the SU(2) spin symmetry, the momentum-averaged spectral weights of the spin-0 and spin-1 states for $\omega>0$ from the spin-1/2 ground state can be shown to be $\delta/4$ and $3\delta/4$, respectively, in the $t$-$J$ model.

This characteristic of the $t$-$J$ model can also be derived using the ground-state wavefunction as follows. The momentum-averaged spectral weight for $\omega>0$ can be expressed as the spectral

weight at a site in a translationally invariant system:

$$\rho_+ = \frac{1}{2N_\mathrm{s}} \sum_{\sigma,m,i} \int_{+0}^{\infty} d\omega |\langle m|\tilde{c}^\dagger_{\boldsymbol{k}_i,\sigma}|\mathrm{GS}\rangle_h|^2 \delta(\omega - \varepsilon_m) = \frac{1}{2} \sum_\sigma {}_h\langle \mathrm{GS}|\tilde{c}_{0,\sigma}\tilde{c}^\dagger_{0,\sigma}|\mathrm{GS}\rangle_h,$$

where $\tilde{c}^\dagger_{0,\sigma}$ denotes the electron creation operator with the no-double-occupancy constraint at site 0. The ground state with spin 1/2 and magnetization $\varsigma$ can be expressed as $|\mathrm{GS}\rangle_h = \sum_{\alpha,\beta} \psi_{\alpha,\beta} |\alpha\rangle^0 \otimes |\beta_\alpha\rangle$, where $|\alpha\rangle^0$ denotes the state with spin $|\alpha|$ and magnetization $\alpha$ ($\alpha = 0$, $1/2$, or $-1/2$) at site 0, and $|\beta_\alpha\rangle$ represents a state with spin $1/2 \pm \alpha$ and magnetization $\varsigma - \alpha$ for the other sites. Because $\tilde{c}^\dagger_{0,\sigma}|\alpha\rangle^0 = \delta_{\alpha,0}|\sigma\rangle^0$, $\tilde{c}^\dagger_{0,\sigma}|\mathrm{GS}\rangle_h = \sum_\beta \psi_{0,\beta}|\sigma\rangle^0 \otimes |\beta_0\rangle$, where $|\beta_0\rangle$ has spin 1/2 and magnetization $\varsigma$. As mentioned above, $\tilde{c}^\dagger_{0,\varsigma}|\mathrm{GS}\rangle_h (= \sum_\beta \psi_{0,\beta}|\varsigma\rangle^0 \otimes |\beta_0\rangle)$ is a spin-1 state with magnetization $2\varsigma$ ($|\mathcal{T}_{2\varsigma}\rangle$). On the other hand, $\tilde{c}^\dagger_{0,-\varsigma}|\mathrm{GS}\rangle_h$ can be expressed as $\frac{1}{\sqrt{2}}(|\mathcal{S}\rangle + |\mathcal{T}_0\rangle)$, where $|\mathcal{S}\rangle = \sum_\beta \psi_{0,\beta}(|-\varsigma\rangle^0 \otimes |\beta_0\rangle - |\varsigma\rangle^0 \otimes |\bar{\beta}_0\rangle)/\sqrt{2}$ and $|\mathcal{T}_0\rangle = \sum_\beta \psi_{0,\beta}(|-\varsigma\rangle^0 \otimes |\beta_0\rangle + |\varsigma\rangle^0 \otimes |\bar{\beta}_0\rangle)/\sqrt{2}$. Here, $|\bar{\beta}_0\rangle = \sum_{i\neq 0} S_i^{+,-\varsigma}|\beta_0\rangle$, which has spin 1/2 and magnetization $-\varsigma$. Then, $|\mathcal{S}\rangle$ and $|\mathcal{T}_0\rangle$ are a spin-0 state and a spin-1 state with magnetization 0, respectively. Because ${}^0\langle\varsigma| - \varsigma\rangle^0 = \langle\bar{\beta}_0|\beta_0\rangle = \langle\mathcal{S}|\mathcal{T}_0\rangle = 0$, $\langle\mathcal{S}|\mathcal{S}\rangle = \langle\mathcal{T}_0|\mathcal{T}_0\rangle = {}_h\langle\mathrm{GS}|\tilde{c}_{0,-\varsigma}\tilde{c}^\dagger_{0,-\varsigma}|\mathrm{GS}\rangle_h$. Here, because ${}_h\langle\mathrm{GS}|\tilde{c}_{0,\varsigma}\tilde{c}^\dagger_{0,\varsigma}|\mathrm{GS}\rangle_h = {}_h\langle\mathrm{GS}|\tilde{c}_{0,-\varsigma}\tilde{c}^\dagger_{0,-\varsigma}|\mathrm{GS}\rangle_h$, the spectral weight of the spin-1 states with magnetization 0 and $2\varsigma$ ($\langle\mathcal{T}_0|\mathcal{T}_0\rangle/4 + \langle\mathcal{T}_{2\varsigma}|\mathcal{T}_{2\varsigma}\rangle/2$) is three times as large as that of the spin-0 state ($\langle\mathcal{S}|\mathcal{S}\rangle/4$). Because $\rho_+ = \delta$ [26, 27], the spectral weights of the spin-0 and spin-1 states for $\omega > 0$ from the spin-1/2 ground state are $\delta/4$ and $3\delta/4$, respectively, in the $t$-$J$ model.

According to this theorem, 3/4 of the total spectral weight for $\omega > 0$ from $|\mathrm{GS}\rangle_1$ with spin 1/2 is due to the spin-1 states in the $t$-$J$ model. In addition, the spectral weight due to $|\mathrm{GS}\rangle_0$ with spin 0 from $|\mathrm{GS}\rangle_1$ with spin 1/2, which corresponds to the spectral weight at the top of the LHB at $N_\mathrm{h} = 0$, usually makes a relatively large contribution to the remaining 1/4. Thus, the spectral weights of the doping-induced states at $N_\mathrm{h} = 1$, which spread over a wide momentum range essentially along the momentum-shifted magnetic dispersion relation, should be primarily due to the spin-1 states (magnetically excited states at half-filling) in the $t$-$J$ model.

Because the low-energy spectral properties of the Hubbard model in the large-$U/t$ regime for $\omega > 0$ are similar to those of the $t$-$J$ model in the small-$J/t$ regime [15, 17], the doping-induced states of the large-$U/t$ Hubbard model in the small-doping limit are also expected to be primarily due to the magnetically excited states at half-filling.

## 5 Spectral functions of the 1D and 2D $t$-$J$ models

To confirm the above picture, we study the spectral functions of the 1D and 2D $t$-$J$ models.

Figure 1(a) shows the results for the 1D $t$-$J$ model at $N_\mathrm{h} = 2$ in a 120-site cluster obtained using the non-Abelian dynamical density-matrix renormalization group method [17, 18], where 120 density-matrix eigenstates are retained. The results imply that the dispersing mode for $\omega > 0$ exhibits essentially the same dispersion relation as the spin-wave mode of the 1D Heisenberg model [22] but shifted by the Fermi momentum, $\omega = -v_\mathrm{1D}\cos k$, for $|k - \pi| < \pi/2$ in the small-doping limit, where $v_\mathrm{1D}$ denotes the spin-wave velocity of the 1D Heisenberg model ($v_\mathrm{1D} = \pi J/2$ [22]); the bandwidth of this mode behaves essentially as $v_\mathrm{1D}$ [inset of Fig. 1(a)]. The spectral weight of this mode gradually disappears toward the Mott transition because $\rho_+ = \delta$ [26, 27] (Sec. 4). Thus, the results for the 1D $t$-$J$ model are consistent with the present picture.

For the 2D $t$-$J$ model, the results in 16-site and 18-site clusters at $N_\mathrm{h} = 1$ obtained using exact diagonalization are shown in Fig. 1(b), where the lowest-energy states with $(-\pi/2, -\pi/2)$ and $(0, -2\pi/3)$ are chosen as the ground states of 16-site and 18-site clusters, respectively,

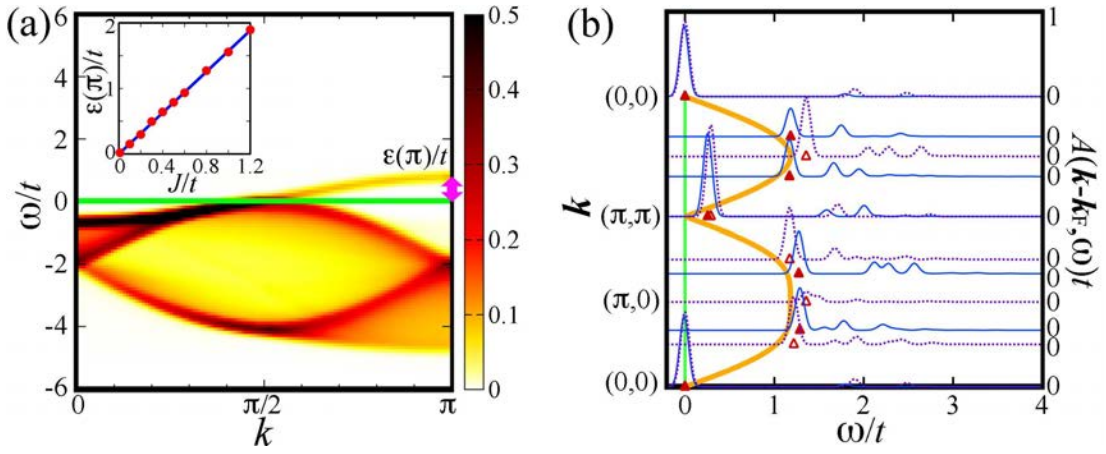


Figure 1: (a) $A(k,\omega)t$ of the 1D $t$-$J$ model for $J/t = 0.5$ at $N_{\rm h} = 2$ in a 120-site cluster. Gaussian broadening with a standard deviation of $0.1t$ is used. In the inset, the red circles show $\varepsilon(\pi)/t$ (pink arrow at $k = \pi$). The blue line indicates $v_{\rm 1D}/t$ with the spin-wave velocity of the 1D Heisenberg model $v_{\rm 1D} = \pi J/2$ [22]. (b) $A(\boldsymbol{k} - \boldsymbol{k}_F, \omega)t$ of the 2D $t$-$J$ model for $J/t = 0.5$ at $N_{\rm h} = 1$ in an 18-site cluster (solid blue curves) and a 16-site cluster (dotted purple curves). Filled and open red triangles indicate the lowest energies at each $\boldsymbol{k}$ measured from the ground-state energies at $N_{\rm h} = 0$ in 18-site and 16-site clusters, respectively. The orange curve indicates the spin-wave dispersion relation of the 2D Heisenberg model in the spin-wave theory: $\omega = \sqrt{2} v_{\rm 2D} \sqrt{1 - [(\cos k_x + \cos k_y)/2]^2}$ [23] with $v_{\rm 2D} \approx 1.18\sqrt{2}J$ [29]. Gaussian broadening with a standard deviation of $0.05t$ is used. The green lines in (a) and (b) indicate $\omega = 0$.

among degenerate ground states. These momenta are labeled as $\boldsymbol{k}_{\rm F}$. The value of $\mu$ is set such that the ground-state energies at $N_{\rm h} = 0$ and 1 are the same. As shown in Fig. 1(b), $A(\boldsymbol{k} - \boldsymbol{k}_{\rm F}, \omega)$ for $\omega > 0$ at $N_{\rm h} = 1$ has significant spectral weights at $\omega$ corresponding to the lowest-energy states of the 2D Heisenberg model at each $\boldsymbol{k}$ [Fig. 1(b), red triangles] for $\boldsymbol{k} - \boldsymbol{k}_{\rm F}$ primarily outside the free-electron Fermi surface; the lowest-energy states at each $\boldsymbol{k}$ are spin-1 states except for those at $\boldsymbol{k} = (0, 0)$ which are the ground states (spin 0) at $N_{\rm h} = 0$. Because these spin-1 states will form the spin-wave mode in the large-cluster limit, these states should form a mode of the doping-induced states which exhibits essentially the spin-wave dispersion relation shifted by the Fermi momentum in the electron-addition spectrum at $N_{\rm h} = 1$ in the large-cluster limit, as indicated by the orange curve in Fig. 1(b). Because the spin-wave mode is gapless [23], the mode of the doping-induced states should also be gapless. Thus, the results for the 2D $t$-$J$ model in 16-site and 18-site clusters are also consistent with the present picture.

Although the data in Fig. 1(b) are essentially the same as those in Ref. [13], the interpretations are different. In the present interpretation, the reason why most of the spin-1 states having significant spectral weights appear in the large-$\omega$ regime ($\omega/t \gtrsim 1$ for $J/t = 0.5$) is simply because the number of $\boldsymbol{k}$ points is small. If the number of $\boldsymbol{k}$ points increases, spin-1 states should appear also in the small-$\omega$ regime for $\omega > 0$ essentially along the momentum-shifted spin-wave dispersion relation, reflecting the gapless spin-wave mode of the 2D Heisenberg model. Note that the low-energy spin-1 states at $\boldsymbol{k} = (\pi, \pi)$ have significant spectral weights in both 16-site and 18-site clusters [Fig. 1(b)]. In Ref. [13], on the other hand, because most of the spin-1 states having significant spectral weights appear in the

large-$\omega$ regime, these states have been interpreted as shakeoff bands disconnected from the low-energy states. Similarly, in a number of studies based on small-cluster calculations, the doping-induced states have been considered to be disconnected from the low-energy states not only in the 2D $t$-$J$ model [13, 30, 31] but also in the 2D Hubbard model [8, 14, 32]; various interpretations different from the present picture have been proposed [8, 13, 14, 30, 32].

# 6 Summary

The relationships between the doping-induced states in the small-doping limit and the magnetically excited states at half-filling were clarified in the $t$-$J$ model. The analysis of the overlaps between these states as well as the analysis of the ratio between the electron-addition spectral weights of the spin-0 and spin-1 states from the spin-1/2 ground state suggests that the doping-induced states in the small-doping limit of a continuous Mott transition can generally be interpreted as essentially the magnetically excited states of the Mott insulator which appear primarily outside the free-electron Fermi surface in the electron-addition spectrum with the dispersion relation shifted by the Fermi momentum following the doping of the Mott insulator, as suggested in Ref. [18]; in the 1D and 2D $t$-$J$ and Hubbard models, because the dispersion relation of the spin-wave mode at half-filling is gapless [22, 23], that of the doping-induced states in the small-doping limit should also be gapless. The numerical results for the 1D and 2D $t$-$J$ models shown in this paper as well as those for the 1D and 2D Hubbard and 2D $t$-$J$ models in Refs. [15, 16, 17, 20] are consistent with this picture.

# Acknowledgments

This work was supported by KAKENHI (Grants No. 23540428 and No. 26400372) and the World Premier International Research Center Initiative (WPI), MEXT, Japan.

# References

[1] H. Eskes, M. B. J. Meinders, and G. A. Sawatzky. Anomalous transfer of spectral weight in doped strongly correlated systems. *Phys. Rev. Lett.*, 67:1035, 1991.

[2] E. Dagotto, A. Moreo, F. Ortolani, J. Riera, and D. J. Scalapino. Density of states of doped Hubbard clusters. *Phys. Rev. Lett.*, 67:1918, 1991.

[3] H. Romberg, M. Alexander, N. Nücker, P. Adelmann, and J. Fink. Electronic structure of the system $La_{2-x}Sr_xCuO_{4+\delta}$. *Phys. Rev. B*, 42:8768, 1990.

[4] C. T. Chen, F. Sette, Y. Ma, M. S. Hybertsen, E. B. Stechel, W. M. C. Foulkes, M. Schulter, S-W. Cheong, A. S. Cooper, L. W. Rupp, B. Batlogg, Y. L. Soo, Z. H. Ming, A. Krol, and Y. H. Kao. Electronic states in $La_{2-x}Sr_xCuO_{4+\delta}$ probed by soft-x-ray absorption. *Phys. Rev. Lett.*, 66:104, 1991.

[5] T. Takahashi, T. Watanabe, T. Kusunoki, and H. Katayama-Yoshida. Angle-resolved photoemission and inverse photoemission studies of $Bi_2Sr_2Ca_{1-x}Cu_2O_8$ ($x = 0, 0.4, 0.6$). *J. Phys. Chem. Solids*, 52:1427, 1991.

[6] M. Imada, A. Fujimori, and Y. Tokura. Metal-insulator transitions. *Rev. Mod. Phys.*, 70:1039, 1998.

[7] E. Dagotto. Correlated electrons in high-temperature superconductors. *Rev. Mod. Phys.*, 66:763, 1994.

[8] S. Sakai, Y. Motome, and M. Imada. Evolution of Electronic Structure of Doped Mott Insulators: Reconstruction of Poles and Zeros of Green's Function. *Phys. Rev. Lett.*, 102:056404, 2009.

[9] Y. Yamaji and M. Imada. Composite-Fermion Theory for Pseudogap, Fermi Arc, Hole Pocket, and Non-Fermi Liquid of Underdoped Cuprate Superconductors. *Phys. Rev. Lett.*, 106:016404, 2011.

[10] Y. Yamaji and M. Imada. Composite fermion theory for pseudogap phenomena and superconductivity in underdoped cuprate superconductors. *Phys. Rev. B*, 83:214522, 2011.

[11] P. Phillips, T.-P. Choy, and R. G Leigh. Mottness in high-temperature copper-oxide superconductors. *Rep. Prog. Phys.*, 72:036501, 2009.

[12] P. Phillips. *Colloquium* : Identifying the propagating charge modes in doped Mott insulators. *Rev. Mod. Phys.*, 82:1719, 2010.

[13] R. Eder and Y. Ohta. Inverse photoemission in strongly correlated electron systems. *Phys. Rev. B*, 54:3576, 1996.

[14] R. Eder, K. Seki, and Y. Ohta. Self-energy and Fermi surface of the two-dimensional Hubbard model. *Phys. Rev. B*, 83:205137, 2011.

[15] M. Kohno. Mott Transition in the Two-Dimensional Hubbard Model. *Phys. Rev. Lett.*, 108:076401, 2012.

[16] M. Kohno. Relationship between Single-Particle Excitation and Spin Excitation at the Mott Transition. *JPS Conf. Proc.*, 3:013020, 2014.

[17] M. Kohno. Spectral properties near the Mott transition in the two-dimensional $t$-$J$ model. *Phys. Rev. B*, 92:085128, 2015.

[18] M. Kohno. States induced in the single-particle spectrum by doping a Mott insulator. *Phys. Rev. B*, 92:085129, 2015.

[19] M. Kohno. Spectral properties near the Mott transition in the two-dimensional Hubbard model with next-nearest-neighbor hopping. *Phys. Rev. B*, 90:035111, 2014.

[20] M. Kohno. Spectral Properties near the Mott Transition in the One-Dimensional Hubbard Model. *Phys. Rev. Lett.*, 105:106402, 2010.

[21] P. Nozières. *Theory of Interacting Fermi Systems.* W. A. Benjamin, New York, 1964.

[22] J. des Cloizeaux and J. J. Pearson. Spin-Wave Spectrum of the Antiferromagnetic Linear Chain. *Phys. Rev.*, 128:2131, 1962.

[23] P. W. Anderson. An Approximate Quantum Theory of the Antiferromagnetic Ground State. *Phys. Rev.*, 86:694, 1952.

[24] P. Prelovšek and A. Ramšak. Spectral functions and the pseudogap in the $t-J$ model. *Phys. Rev. B*, 63:180506, 2001.

[25] M. Kohno. Ground-state properties of the two-dimensional $t$-$J$ model. *Phys. Rev. B*, 55:1435, 1997.

[26] W. Stephan and P. Horsch. Fermi surface and dynamics of the $t$ - $J$ model at moderate doping. *Phys. Rev. Lett.*, 66:2258, 1991.

[27] E. Dagotto, A. Moreo, F. Ortolani, D. Poilblanc, and J. Riera. Static and dynamical properties of doped Hubbard clusters. *Phys. Rev. B*, 45:10741, 1992.

[28] K. Penc, K. Hallberg, F. Mila, and H. Shiba. Spectral functions of the one-dimensional Hubbard model in the $U\rightarrow+\infty$ limit:How to use the factorized wave function. *Phys. Rev. B*, 55:15475, 1997.

[29] R. R. P. Singh and D. A. Huse. Microscopic calculation of the spin-stiffness constant for the spin-$\frac{1}{2}$ square-lattice Heisenberg antiferromagnet. *Phys. Rev. B*, 40:7247, 1989.

[30] R. Eder, Y. Ohta, and T. Shimozato. Validity of the rigid-band picture for the $t$ - $J$ model. *Phys. Rev. B*, 50:3350, 1994.

[31] T. Tohyama. Asymmetry of the electronic states in hole- and electron-doped cuprates: Exact diagonalization study of the $t$-$t^{'}$-$t^{''}$-$J$ model. *Phys. Rev. B*, 70:174517, 2004.

[32] S. Sakai, Y. Motome, and M. Imada. Doped high-$T_c$ cuprate superconductors elucidated in the light of zeros and poles of the electronic Green's function. *Phys. Rev. B*, 82:134505, 2010.